

JP1.10 A NOVEL APPROACH TO MARINE WIND SPEED ASSESSMENT USING SYNTHETIC APERTURE RADAR

Todd D. Sikora^{*}

Millersville University, Department of Earth Sciences, Millersville, Pennsylvania

George S. Young

Pennsylvania State University, Department of Meteorology, University Park, Pennsylvania

Nathaniel S. Winstead

Johns Hopkins University, Applied Physics Laboratory, Laurel, Maryland

1. INTRODUCTION

Given the sparse in situ data network in most marine regions, mariners and operational weather forecasters have relied heavily on remotely sensed data, such as scatterometers, in order to assess the state of marine meteorological conditions, including the near-surface wind vector. Scatterometers operate on the premise that microwave normalized radar cross section (NRCS) of the ocean surface is related to the wind vector (e.g., Stoffelen and Anderson 1997). Typical scatterometers have order of magnitude 10 km resolution and land contamination precludes their use in a resolution-size band directly adjacent to the shore.

Recent research has proven that NRCS from space borne synthetic aperture radar (SAR) can be used to produce marine wind speed fields that are comparable to those provided by scatterometers (e.g., Horstmann et al. 2003; Monaldo et al. 2004). The resolution of SAR is several orders of magnitude higher than that of scatterometers. Thus, SAR has the potential to provide detail in wind speed fields beyond that available from scatterometers and to provide coastal wind speed fields where scatterometers fail.

A major obstacle to SAR-based wind speed retrieval is the requirement for a priori knowledge of the wind direction. The inversion between normalized radar cross section (NRCS) and wind speed is not unique because at moderate incident angles and wind speeds, any one value of NRCS can correspond to several wind speed / wind direction pairs. Scatterometers reduce this uncertainty by sensing a given area of ocean surface with multiple antennae.

Researchers aiming to produce SAR-based wind speed fields have employed scatterometer wind directions (e.g., Monaldo et al. 2004), numerical model wind directions (e.g., Monaldo et al. 2001), and the SAR-signatures of linear geophysical features assumed to be aligned with the wind direction (e.g., Horstmann et al. 2000).

Each of the above-mentioned wind direction estimation techniques has potential shortcomings, especially in coastal regions. As mentioned earlier, scatterometer wind data have a much coarser resolution

than SAR data and are not available close to coastlines. Operational numerical model data are typically at least as coarse as scatterometer data and mesoscale and microscale interpretations of such data are often suspect. Finally, linear features may be absent on SAR images or, if present, may not be aligned with the wind direction.

The objective of this paper is to propose a product that allows one to assess the lower and upper bounds on SAR-based wind speed. Although this product could be generated for any marine SAR scene, we envision it to be most useful in coastal regions where the large concentration of maritime operations requires accurate, high-resolution wind speed data and when the above-mentioned wind direction uncertainties preclude the generation of accurate SAR-based wind speed data. This paper represents a condensed version of a complementary paper of the same title and authorship currently in press at *Weather and Forecasting*.

2. METHODOLOGY

We will focus on a wind speed assessment product based on ScanSAR Wide data from the SAR onboard the Canadian Space Agency's RADARSAT-1. That SAR is C-band (5.6 cm) and right-looking with horizontal-horizontal polarization. Our SAR-based wind speed fields are generated following the methodology outlined in Section II of Monaldo et al. (2004). In particular, we use the GMF known as CMOD4 (Stoffelen and Anderson 1997) modified for horizontal-horizontal polarization using a polarization parameter of 0.6.

To produce our wind speed assessment product, we generate two SAR-based wind speed images. One image is generated using a wind direction opposite to the radar look direction. The other image is generated using a wind direction perpendicular to the radar look direction. For a given value of NRCS, the former produces the minimum value of wind speed and the latter produces the maximum value of wind speed for moderate incident angles and wind speed conditions. For the current research, we've chosen to use 600 m pixels.

To provide the reader with a conventional estimate of SAR-based wind speed field in the case study presented below, we show a SAR-based wind speed image using a wind direction field from the United States

^{*}Corresponding author address: Todd D. Sikora, Millersville University, Department of Earth Sciences, Millersville, Pennsylvania, 17551. Email: Todd.Sikora@millersville.edu

Navy's NOGAPS model. This is the primary wind direction technique used at the Johns Hopkins University Applied Physics Laboratory for the production of their on-line SAR-based wind speed data. In doing so, we will identify several likely areas of wind direction error by NOGAPS.

3. CASE STUDY

3.1 Meteorological setting

We will demonstrate our procedure on a case involving coincident synoptic scale and mesoscale marine meteorological events over the northern Gulf of Alaska. The SAR image for this case (not shown) was taken at 0310 UTC 18 February 2000. The corresponding surface synoptic analysis from the National Centers for Environmental Prediction is provided in Figure 1. The available coastal, ship, and

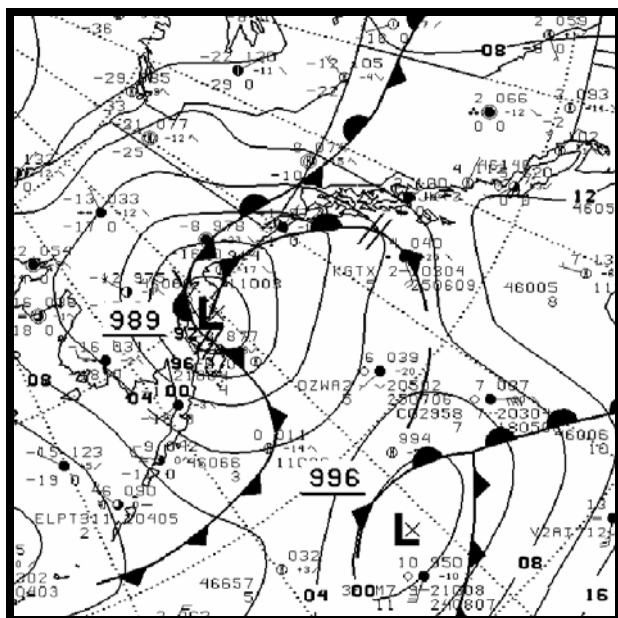


Figure 1. Surface analysis from the National Centers for Environmental Prediction for 0000 UTC 18 February 2000. A synoptic scale cyclone is analyzed over the northwest Gulf of Alaska with a surface front extending east and then southeastward near the Alaskan coast.

buoy observations, coupled with conventional meteorological satellite data, are just sufficient to allow the analyst to determine that a strong synoptic scale cyclone is present over the northern Gulf of Alaska and that some form of meteorological boundary extends in a general eastward direction from the cyclone's center, roughly paralleling the Alaskan coast.

As will be shown in the next subsection, that boundary is the seaward edge of a mesoscale barrier jet and thus is associated with a sharply defined band of markedly larger cyclonic winds directly adjacent to the coast (e.g., Overland and Bond 1993; Loescher et al. in press).

3.2. Results

The SAR-based wind speed field resulting from the use of NOGAPS wind directions is shown in Figure 2.

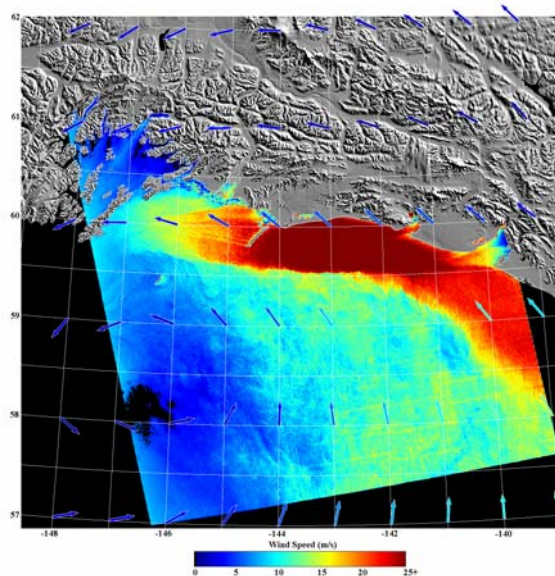


Figure 2. SAR-based wind speed image of the northeast Gulf of Alaska at 0310 UTC 18 February 2000, based on the NOGAPS wind direction field.

The colored arrows found at the latitude-longitude intersections in Figure 2 represent the NOGAPS wind vector field. These NOGAPS wind vectors are 6-hour forecasts from the model's 0000 UTC 18 February 2000 run. According to NOGAPS, a synoptic scale cyclone is located to the west of the image. Analysis of the SAR image using the techniques provided in Young et al. (2005), however, indicates that the cyclone is actually centered at about 58.25 N, 146.50 W. According to NOGAPS, the cyclone is producing southerly and southeasterly flow towards the coast throughout most of the imaged area.

The resulting SAR-based wind speed is 5.0 to 15.0 $m s^{-1}$ over most of the southwestern portion of the image, with the wind speed decreasing towards the cyclone's center. However, directly adjacent to the Alaskan coastline, a sharply defined 50 km wide band of markedly larger wind speed is found. This band is a mesoscale barrier jet (Loescher et al. in press). Although not resolved by NOGAPS, the likely wind direction within the barrier jet is cyclonic, mainly paralleling the shore (Overland and Bond 1993). Note that the SAR-based wind speed is $\geq 25.0 m s^{-1}$ over much of the jet's length. Of particular interest is the sharp jump in wind speed along the seaward edge of the barrier jet. Moreover, the wind speed image reveals smaller, 15.0 to 25.0 $m s^{-1}$ gap flow jets (e.g., Macklin et al. 1990) that appear, by their orientation, to feed out of the two bays near 60.00 N, 141.50 W (Icy Bay) and 59.75 N, 140.00 W (Yakutat Bay), and merge into the barrier jet. The likely gap flow wind directions are also not resolved by NOGAPS.

Recall that we have documented several likely areas of wind direction forecast error by NOGAPS for this case study. The range of SAR-based wind speed that could result from the incorrect forecast of the wind direction can be seen by comparing Figures 3 and 4.

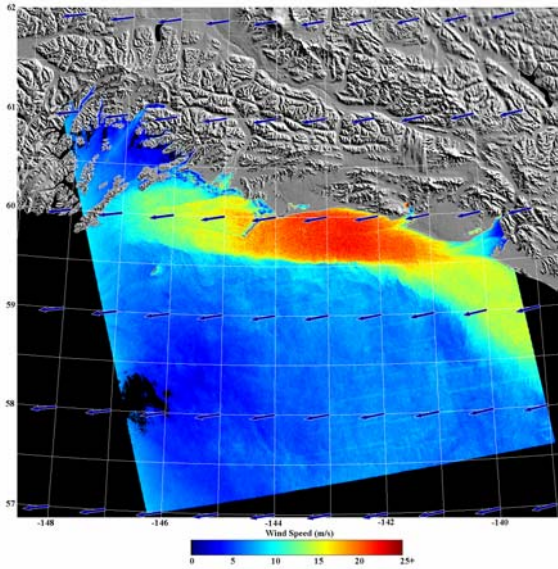


Figure 3. SAR-based wind speed image of the northeast Gulf of Alaska at 0310 UTC 18 February 2000, based on an assumed wind direction field opposite to the radar look direction.

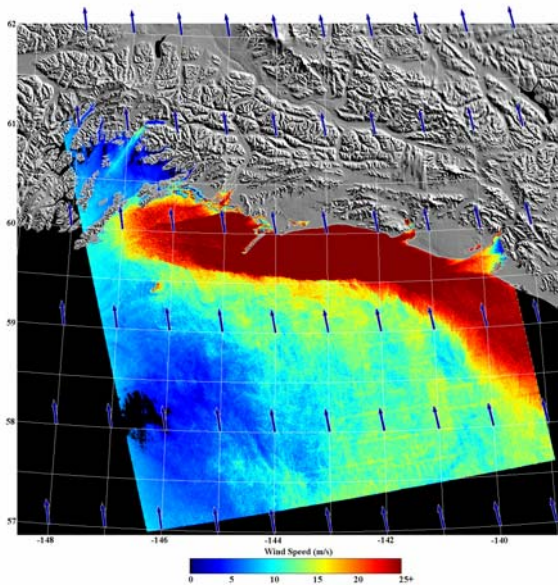


Figure 4. SAR-based wind speed image of the northeast Gulf of Alaska at 0310 UTC 18 February 2000, based on an assumed wind direction field perpendicular to the radar look direction.

4. The blue arrows found at the latitude-longitude intersections in Figures 3 and 4 represent the constant wind direction fields we impose (080° and 170° from true north, respectively). Figure 3 presents the minimum SAR-based wind speed field while Figure 4

presents the maximum SAR-based wind speed field. These two figures provide the lower and upper bounds on the wind speed field consistent with the SAR data.

As can be seen by comparing Figures 2, 3, and 4, the SAR-based estimates of surface wind speed can lie anywhere in this range of direction-dependent possibilities. Where the true wind direction is mainly opposite to the radar look direction—as in the center portion of the barrier jet, the two gap flows, and that portion of the synoptic wind field north of the cyclone's center—the true wind speed will be near the lower limit. As evidence of this, NDBC Station 46061, located at 60.22° N, 146.83° W, reported a wind direction of 076° from true north and a wind speed of 10.8 m s^{-1} at 0300 UTC 18 February 2000, almost exactly matching the wind information found at 60.22° N, 146.83° W on Figure 3. Where the wind direction is mainly perpendicular to the radar look direction—as in the eastern portion of the barrier jet and that portion of the synoptic wind field east of the cyclone's center—the true wind speed will be near the upper limit. Where reliable automated wind direction information is unavailable, prudence dictates one assume that the wind speeds depicted on Figure 4 are at least possible.

4. SUMMARY AND RECOMMENDATIONS

This paper describes and demonstrates a high-resolution (order of magnitude 0.1 km to 1 km) wind speed assessment product based on SAR. The product allows one to assess the bounds on SAR-based wind speed, on a pixel-by-pixel basis, using scatterometry techniques. Simply put, the minimum SAR-based wind speed at each pixel is produced by setting the wind direction at each pixel to be opposite to the radar look direction. In contrast, the maximum SAR-based wind speed at each pixel is produced by setting the wind direction at each pixel to be perpendicular to the radar look direction.

We envision the assessment product to be most useful in coastal regions where the large concentration of maritime operations requires accurate, high-resolution wind speed data and when wind direction errors preclude the generation of accurate SAR-based wind speed data.

Acknowledgments. This research was supported by Office of Naval Research grants N00014-04-WR20365, N00014-04-10539, and N00014-05-WR20319 as well as National Science Foundation grant ATM-0240869. We thank Frank M. Monaldo and Donald R. Thompson for the technical assistance they provided in the preparation of this manuscript.

5. REFERENCES

Horstmann, J., W. Koch, S. Lehner, and R. Tonboe, 2000: Wind retrieval over the ocean using synthetic aperture radar with C-band HH polarization. *IEEE Trans. Geosci. Remote Sens.*, **38**, 2122-2131.

- Horstmann, J., J. Schiller, J. Schulz-Stellenfleth, and S. Lehner, 2003: Global wind speed retrieval from SAR. *IEEE Trans. Geosci. Remote Sens.*, **41**, 2277 – 2286.
- Loescher, K. A., G. S. Young, B. A. Colle, and N. S. Winstead, 2005: Climatology of barrier jets along the Alaskan coast, Part 1: Spatial and temporal distribution. *Mon. Wea. Rev.*, in press.
- Macklin, S. A., N. A. Bond, and J. P. Walker, 1990: Structure of a low-level jet over lower Cook Inlet, Alaska. *Mon. Wea. Rev.*, **118**, 2568-2578.
- Monaldo, F. M., D. R. Thompson, R. C. Beal, W. G. Pichel, and P. Clemente-Colón, 2001: Comparison of SAR-derived wind speed with model predictions and ocean buoy measurements. *IEEE Trans. Geosci. Remote Sens.*, **39**, 2587-2600.
- Monaldo, F. M., D. R. Thompson, W. G. Pichel, and P. Clemente-Colón, 2004: A systematic comparison of QuikSCAT and SAR ocean surface wind speeds. *IEEE Trans. Geosci. Remote Sens.*, **42**, 283 – 291.
- Overland, J. E. and N. A. Bond, 1993: The influence of coastal orography: The Yakutat storm. *Mon. Wea. Rev.*, **121**, 1388-1397.
- Stoffelen, A. and D. Anderson, 1997: Scatterometer data interpretation: Estimation and validation of the transfer function CMOD4. *J. Geophys. Res.*, **102**, 5767-5780.
- Young, G. S., T. D. Sikora, and N. S. Winstead, 2005: Use of synthetic aperture radar in fine-scale surface analysis of synoptic-scale fronts at sea. *Wea. Forecasting*, **20**, 311-327.